

MRAO-1900
DAMTP-96-11
Submitted to *PRL*
February 1996

Cosmic Microwave Background experiments targeting the cosmic strings Doppler peak signal

Joao Magueijo^{1,2}, Mike P. Hobson²

⁽¹⁾Department of Applied Mathematics and Theoretical Physics, University of Cambridge,
Cambridge CB3 9EW, U.K.

⁽²⁾Mullard Radio Astronomy Observatory, Cavendish Laboratory, Madingley Road, Cambridge,
CB3 0HE, U.K.

Abstract

We investigate which experiments are better suited to test the robust prediction that cosmic strings do not produce secondary Doppler peaks. We propose a statistic for detecting oscillations in the C^l spectrum, and study its statistical relevance given the truth of an inflationary competitor to cosmic strings. The analysis is performed for single-dish experiments and interferometers, subject to a variety of noise levels and scanning features. A high resolution of 0.2 degrees is found to be required for single-dish experiments with realistic levels of noise. Interferometers appear to be more suitable for detecting this signal.

In two recent *Letters* [1, 2] it was shown how the existence or absence of secondary Doppler peaks in the cosmic microwave background (CMB) power spectrum C^l could rule out or confirm a large class of defect theories, including cosmic strings. The argument used is attractive in that it does not depend on details of defects or inflation, but only makes use of well-established contrasting properties peculiar to the two types of theory. This is particularly welcome when calculations in defect scenarios are so difficult and unreliable. A simple but robust test based on an issue about to be decided by experiment seems a soundly cautious approach to defect theories.

The question therefore arises: which CMB experiments can resolve the secondary Doppler peaks? This is a timely issue when so many proposals for ground based and satellite borne CMB experiments are being made [3]. Experimental features have so far been motivated by their implications on inflationary parameter fixing from Doppler peaks' position, height, and shape [4, 5]. Secondary peak detection is a far less demanding task, and can be used to quantify experimental spectral resolution at the most basic level. In [6] we analyze this problem in a general setting, but here we consider only its bearings on cosmic string theories.

Apart from the absence of secondary Doppler peaks in cosmic string theories, the only reliable feature known is that their primary peak is located at $l = 400 - 600$. If the main peak is measured outside this range one can rule out cosmic strings, but we shall assume here that this is not the case. In order to identify experiments targeting the string's lack of secondary oscillations we investigate how we could falsify cosmic strings given the truth of a competitor inflationary scenario with a primary peak located in $l = 400 - 600$ and exhibiting secondary oscillations. For definiteness we have taken CDM with $\Omega = 0.3$, $h = 0.6$, $\Omega_b h^2 = 0.02$, and a flat primordial spectrum. We shall call this theory stCDM, the CDM competitor of cosmic strings, and we plot its C^l spectrum in Fig 1. The main peak height and shape will be assumed to be the same for cosmic strings and stCDM, and the low l section of the spectrum will be ignored. In this way we assume maximal confusion in whatever is uncertain, or alien to the signal to be experimentally tested.

The idea is to apply to stCDM a statistic sensitive only to the existence or absence of secondary oscillations. To set it up, we first compute the average power C_i in bins $i = 1, 2, 3$ denoted by horizontal bars in Fig 1. We then infer the spectrum convexity with $\mathcal{C} = (C_1 + C_3)/2 - C_2$. A positive convexity reflects unambiguously the first dip of the spectrum and therefore the first secondary oscillation. If the overall error in \mathcal{C} is $\sigma(\mathcal{C})$ then one can claim that \mathcal{C} is positive (and therefore that there are secondary oscillations) with a number of sigmas equal to

$$\Sigma = \frac{\langle \mathcal{C} \rangle}{\sigma(\mathcal{C})} . \quad (1)$$

Σ is then to be seen as the stCDM secondary peak detection function, or equivalently, the cosmic string rejection function.

In this *Letter* we set up a large parameter space of experiments, on which we compute the contours of Σ . We consider two types of experiments: single-dish experiments (recovering some of the results in [5]) and interferometers. For single-dish experiments we allow the beam size, sky coverage, and detector noise to vary. For interferometers we take as free parameters the primary beam, number of fields, and detector noise. We consider errors associated with cosmic/sample variance, spectral resolution limitations due to finite sky coverage, and instrumental noise. Foreground subtraction errors are included (not naively, as we prove in [6]) in the form of only an

extra instrumental noise term.

We outline a method for computing errors in C^l estimates explained in more detail and generality in [6]. For simplicity we consider the small field limit, and assume at first no instrumental noise or foreground subtraction uncertainties. We stereographically project the sky onto a plane, and expand in Fourier modes, using the symmetric notation (factors of 2π evenly distributed). We denote by $a(\mathbf{k})$ the modes provided by an all-sky observation with infinite resolution, and $a^s(\mathbf{k})$ the modes as seen through an observation window $W(\mathbf{x})$ and convolved with a beam $B(\mathbf{x})$. For a single-dish experiment we shall assume that the window is a square of side L treated with a cosine bell [7] (to bar edge effects), and that the beam is a Gaussian with FWHM θ_b . For interferometers the window (better known as the primary beam) is a Gaussian with FWHM θ_w , and the beam is essentially unity [8]. Using the convolution theorem twice we have that

$$a^s(\mathbf{k}) = \int \frac{d^2k'}{2\pi} a(\mathbf{k}') B(\mathbf{k}') W(\mathbf{k} - \mathbf{k}') \quad (2)$$

where $W(\mathbf{k})$ is the window Fourier transform. The all-sky modes form a diagonal covariance matrix $\langle a(\mathbf{k}) a^*(\mathbf{k}') \rangle = C(k) \delta(\mathbf{k} - \mathbf{k}')$, where the brackets denote ensemble averages. In calculations concerning small patches of the sky $C(k)$ can be obtained by interpolating the C^l with $k = l$ [6, 9]. On the other hand the sampled modes $a^s(\mathbf{k})$ form the covariance matrix [8]

$$\begin{aligned} \langle a^s(\mathbf{k}) a^{s*}(\mathbf{k}') \rangle = \\ \int \frac{d\mathbf{k}''}{(2\pi)^2} C(\mathbf{k}'') B^2(\mathbf{k}'') W(\mathbf{k} - \mathbf{k}'') W^*(\mathbf{k}' - \mathbf{k}'') \end{aligned} \quad (3)$$

which encodes all the finite sampling hurdles for recovering the power spectrum C^l , now to be examined.

Firstly, the sampled modes power spectrum $C^s(\mathbf{k}) = \langle a^s(\mathbf{k}) a^{s*}(\mathbf{k}) \rangle$ becomes the convolution of the raw power spectrum with the window power spectrum [7, 8, 10, 11]. This has the effect of leaving a low k white noise tail in $C^s(\mathbf{k})$ up to $k \approx 1/L$, and thereafter averaging out oscillations in the raw spectrum on a scale $\Delta l \approx 1/L$. If the field has edges there will also be spurious oscillations of period $1/L$ superposed on the spectrum. Field edges can be treated as in [7]. In the case of a square field the window should be multiplied by a cosine bell. Whenever the sampled spectrum is highly distorted, a deconvolution recipe is then required. In the presence of noise and cosmic/sample variance this induces a large deterioration of the detection function. We have however checked [6] that, providing edge effects are treated, one has in the stCDM Doppler peak region

$$C^s(\mathbf{k}) \approx C(k) B^2(k) \int \frac{d\mathbf{k}'}{(2\pi)^2} |W(\mathbf{k}')|^2 = \alpha C(k) B^2(k) \quad (4)$$

for fields with $L > 4$ degrees, or $\theta_w > 2$ degrees (we illustrate this point in Fig. 1). Therefore, as long as the field is not too small, deconvolution is trivial in the relevant spectrum sections of stCDM, and it does not add any extra errors. Note that $\alpha = \Omega^s / (2\pi)^2$, where Ω^s is the field area ($\Omega^s = L^2$ for a square field, $\Omega^s = \pi \theta_w^2 / (8 \log 2)$ for a primary beam).

Secondly, finite fields have the effect of correlating neighbouring $a^s(\mathbf{k})$ modes within a correlation radius $\xi \approx 1/L$ (assuming edge effects have been treated) or $\xi \approx 1/\omega_w$. This translates into a correlation length $\bar{\xi}(k)$ between $C(k)$ estimates. In [6] we show how spectral resolution

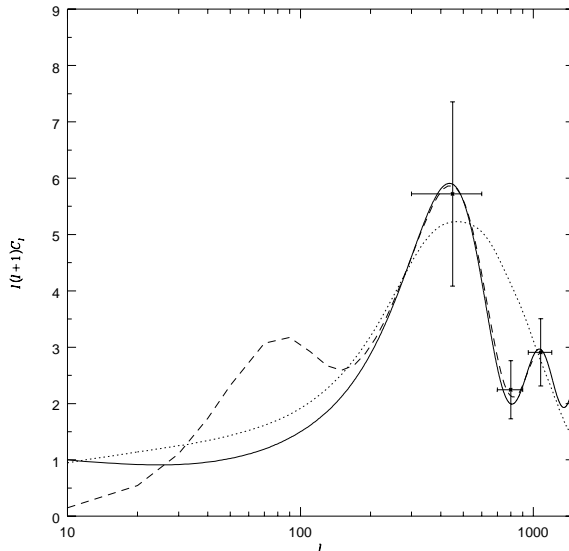


Figure 1: The angular power spectrum of stCDM (line) and one possibility for cosmic strings (points). The dashed curve is the stCDM power spectrum $C^s(k)$ as sampled by an interferometer with $\theta_w = 2^\circ$ (divided by α defined in Eqn. (4)). We have plotted the bins used in \mathcal{C} as horizontal bars, their level indicating the average spectrum in bin. The vertical errorbars are the cosmic/sample variance.

in the Doppler peak region is typically imposed, not by the fact that a given $C(k)$ estimate receives contributions from neighbouring k , but because we can only make uncorrelated estimates of the power spectrum with a separation $\bar{\xi}(k)$. This effect is reminiscent of cosmic covariance in non-Gaussian theories [12]. Correlations also determine the cosmic/sample variance. Using $\text{cov}(x^2, y^2) = 2\text{cov}^2(x, y)$, it can be proved that any power spectrum estimate C_Ω (using a 2D region Ω of the Fourier domain, with area A_k , in which $C^s(\mathbf{k})$ does not vary much) is affected by the sample variance

$$\sigma^2(C_\Omega) = \frac{2C_\Omega^2}{\tilde{N}_\Omega} = 2C_\Omega^2 \int \frac{d\mathbf{k}d\mathbf{k}'}{A_k^2} \text{cor}^2(a^s(\mathbf{k}), a^{s*}(\mathbf{k}')). \quad (5)$$

\tilde{N}_Ω acts as the effective number of independent modes in the region, and it can be used to define an average density of independent modes ρ_0 .

We have found it convenient to replace the \mathbf{k} space by a square mesh, to be called uncorrelated-mesh, with a spacing locally given by $k_0 \approx 1/\sqrt{\rho_0}$. This mesh, on average, contains all the non-redundant information, given cosmic/sample variance and the correlations imposed by finite sampling. We have checked that the uncorrelated-mesh is nearly a square lattice with $k_0 \approx 2\pi/L$ for a square field, and $k_0 \approx 2\sqrt{4\pi \log 2}/\theta_w$ for a Gaussian field. Although it is easy to improve on this approximation, it is normally a good enough recipe. Using only mesh points (denoted by \mathbf{k}_i) the sampled power spectrum $C^s(k)$ can be estimated with

$$C_s(k) = \frac{1}{N_k} \sum_{|\mathbf{k}_i|=k} |a^s(\mathbf{k}_i)|^2 \quad (6)$$

where N_k is the number of modes in the mesh which satisfy $|\mathbf{k}_i| = k$. The residual correlations between these estimates fall below 5%, but only a finite number of k can be estimated. Their average separation $\Delta k \approx \sqrt{k^2 + k_0^2/\pi} - k$, for $k > k_0$, defines the maximal spectral resolution. More estimates could be inserted in between these, but they would necessarily be correlated estimates. Only for $k > k_0^2/(2\pi)$ can individual C^l be estimated ($\Delta k \approx 1$). The cosmic variance in these estimates is approximately $\sigma^2(C_s(k)) \approx 2C^{s2}(k)/N_k$. For $k > k_0^2/(2\pi)$ this means $\sigma^2(C^l) \approx (C^{l2}/l)(4\pi/L^2)$, as naively expected [13]. For $k < k_0^2/(2\pi)$ the naive expectation breaks down.

We now study the effects of noise, differentiating between single-dish experiments and interferometers. Let Ω_{pix} be the pixel area, and σ_{pix}^2 be the noise per pixel [4]. Fixing the detector sensitivity s and total time of observation t_{tot} fixes the quantity $w^{-1} = 4\pi s^2/t_{tot} = \sigma_{pix}^2 \Omega_{pix} (4\pi/L^2)$, which we therefore use to parameterize the noise level. The noise introduces an extra diagonal term with value $\alpha w^{-1} L^2/(4\pi)$ into the mesh modes covariance matrix. Hence a centred uncorrelated-mesh estimator of the power spectrum is now

$$\overline{C}(k) = \left(\frac{1}{N_k \alpha B^2} \sum_{|\mathbf{k}_i|=k} |\alpha^s(\mathbf{k}_i)|^2 \right) - \frac{\sigma_{pix}^2 \Omega_{pix}}{B^2(k)} \quad (7)$$

and its variance is

$$\frac{\sigma^2(\overline{C}(k))}{C^2(k)} = \frac{2}{N_k} \left(1 + \frac{w^{-1} L^2}{4\pi B^2 C(k)} \right)^2 \quad (8)$$

For interferometers [14] noise is added directly in Fourier space. The noise in a given mesh cell is given by $\sigma_N^2 = s^2 \Omega^{s2}/(t_{vis} N_{vis})$, where N_{vis} is the number of visibilities in the cell, s is the sensitivity of the detectors, and t_{vis} is the time spent observing each visibility. The coverage density $\rho_c = N_{vis} t_{vis} \Omega^s/t_f$ (where t_f is the time spent on a given field) is assumed to be uniform in a ring of the uv -plane containing the stCDM relevant bins. This assumes a dish geometry like the one proposed in [15]. If one decides to observe n_f well-separated fields, then each mesh-point acquires an extra index $i = 1, \dots, n_f$, and points with different indices are uncorrelated. For fixed detector sensitivity and total observation time one should now keep constant $w^{-1} = (2\pi)^2 s^2/(\rho_c t_{tot}) = (2\pi)^2 \sigma_N^2/(\Omega^{s3} n_f)$, and so this is the noise parameterization we choose for interferometer estimates. A centred estimator is now

$$\overline{C}(k) = \left(\frac{1}{N_k \alpha} \sum_{|\mathbf{k}_i|=k} |\alpha^s(\mathbf{k}_i)|^2 \right) - \frac{\sigma_N^2}{\alpha} \quad (9)$$

and its variance is

$$\frac{\sigma^2(\overline{C}(k))}{C^2(k)} = \frac{2}{N_k} \left(1 + \frac{w^{-1} \Omega^{s2} n_f}{C(k)} \right)^2 \quad (10)$$

From these results one can compute Σ in the large experiment parameter space proposed (which always assumes $L > 4^\circ$, or $\theta_w > 2^\circ$). Two types of results ensue. Firstly, one can provide guidance on experimental design given a constraint, such as finite funding. This constraint is mathematically translated into hypersurfaces of constant w^{-1} . Secondly, we may provide the value of the detection as a function of w^{-1} , assuming ideal design. This will set lower bounds on w^{-1} for any meaningful detection, telling us thereafter how fast the detection improves with a given w^{-1} improvement.

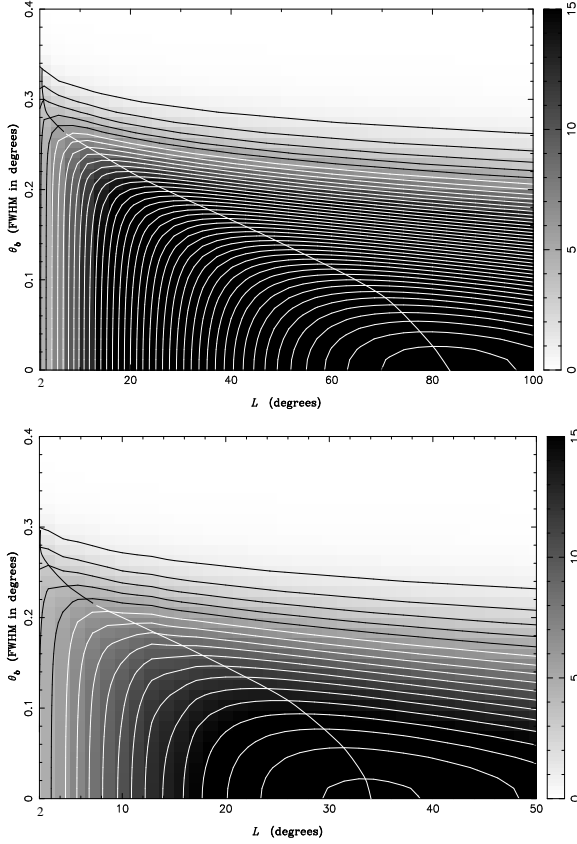


Figure 2: Low noise ($w^{-1} = (25\mu K)^2(^\circ)^2$, top) and high noise ($w^{-1} = (60\mu K)^2(^\circ)^2$, bottom) contours of the $\Sigma(L, \theta_b; w^{-1})$ function for stCDM. We have also plotted the ideal scanning lines $L_i(\theta_b)$.

In Fig. 2 we show a low and a high noise section of $\Sigma(L, \theta_b; w^{-1})$ for single-dish experiments [16]. Most noticeable are the high resolutions required for a significant detection ($\theta_b < 0.3^\circ$ and $\theta_b < 0.25^\circ$, respectively). These are due to the fact that we are testing features at a rather large l , and the noise term goes up exponentially with l as we approach the resolution limit. It is also obvious that all-sky scanning is not ideal under realistic levels of noise. For fixed resolution and noise, increasing the coverage area will at first increase the detection, but beyond a certain coverage L_i , the detection will initially saturate, then start to decrease. This is because noise separation relies on allowing the *same* coherent signal to compete with the incoherent noise. Only after the signal has dominated the noise does it make sense to increase the coverage area, so as to reduce the sample variance. If the noise is very high, then all t_{tot} should possibly be used in a small patch of the sky (larger than 4°). The ideal scanning lines $L_i(\theta_b)$ are plotted in Fig. 2. As the resolution increases so do L_i and the achieved $\Sigma(L_i, \theta_b; w^{-1})$. Initially they increase very fast; then, for $\theta_b < 0.1^\circ$, not by much. For a low noise experiment ($w^{-1} = (25\mu K)^2(^\circ)^2$) the detection increases from $\Sigma = 1$ to $\Sigma \approx 36$ as the resolution is improved from $\theta_b = 0.3^\circ$ to $\theta_b = 0.1$ (with $L_i \approx 4^\circ$ and $L_i \approx 65^\circ$, respectively). From then on Σ improves by only a few sigmas. Even with infinite resolution the ideal coverage area is $L \approx 80^\circ$. For a high noise experiment

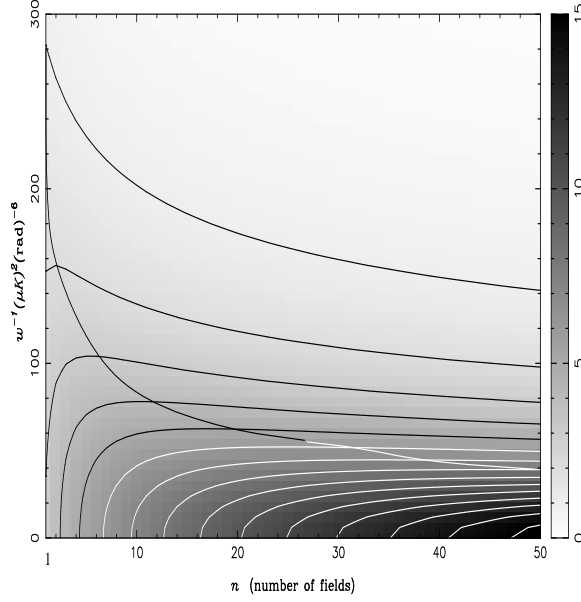


Figure 3: $\Sigma(\theta_w = 2^\circ, n_f; w^{-1})$ contours and density map, and ideal scanning line $n_{fi}(w^{-1})$.

($w^{-1} = (60\mu K)^2(\text{rad})^2$) the resolution is even more crucial. One needs $\theta_b = 0.25^\circ$ to obtain a 3 sigma detection (with $L = 4^\circ$), and a decent $\Sigma = 10$ detection can be achieved only with $\theta_b \approx 0.15^\circ$ (and $L_i = 18^\circ$). It can be checked that all-sky coverage is only useful if the noise is lower than about $w^{-1} = (11\mu K)^2(\text{rad})^2$.

In Fig. 3 we show $\Sigma(\theta_w = 2^\circ, n_f; w^{-1})$ for an interferometer. Ideal scanning now always means $\theta_w = 2^\circ$, and the ideal coverage area is fixed by a curve $n_{fi}(w^{-1})$. The high noise region is $w^{-1} > (150\mu K)^2\text{rad}^{-6}$. There one should look into only one or two 2° fields, in order to obtain a detection between 1 and 2 sigma. For $w^{-1} < (150\mu K)^2\text{rad}^{-6}$ we enter the signal dominated region. Following the ideal scanning line with decreasing w^{-1} , n_{fi} and Σ start increasing, first slowly, then very fast. For $w^{-1} = (100\mu K)^2\text{rad}^{-6}$ one may obtain a 3 sigma detection using 8 independent fields with $\theta_w = 2^\circ$. For $w^{-1} = (20\mu K)^2\text{rad}^{-6}$ it is worth looking into about 40 of these fields, obtaining thus an 8 sigma detection. We have estimated CAT noise level to be $w^{-1} = (300\mu K)^2\text{rad}^{-6}$. This is a mere prototype, and a 10-fold improvement should be easily attained.

These results stress the contradictions of an all-purpose experiment. If the low- l plateau of the spectrum is the theoretical target then one needs all-sky coverage, and satellite single-dish experiments are to be favoured. Even if one wishes to target the main sCDM features, encoded mostly in the first peak's place and height, then this is still true [17]. Our work shows how such a design relies heavily on the assumption that the signal is in the vicinity of sCDM. If instead one is to test the high- l opposition between low Ω CDM and cosmic strings, then we have seen that single-dish experiments are required to have rather high resolutions. Interferometers appear to be less constrained, providing 2-3 sigma detections under very unassuming conditions, with rapid improvements following further experimental condition improvement. Furthermore, in this

context, all-sky scanning is not only unnecessary, but in fact undesirable. The best scanning is normally achieved with deep small patches. These two features contradict sharply the ideal experimental design motivated by the standard theoretical gospel. We believe that a variety of contrasting experimental techniques may equally well find their niche of important theoretical implications.

We should mention, in closing, that if one is to combine the high- l cosmic string signal with the requirement that the low- l section of the spectrum is to be measured, then the logic is naturally changed. See [18] for this alternative perspective.

ACKNOWLEDGEMENTS: J.M. would like to thank A.Albrecht, M.Jones, and B.Wandelt for useful discussions. We thank M.White for supplying the stCDM C^l spectrum. We acknowledge St.John's College (J.M.), and Trinity Hall (M.H.), Cambridge, for support in the form of research fellowships.

References

- [1] A. Albrecht, D. Coulson, P. Ferreira, and J. Magueijo, to be published in *Phy.Rev.Lett.*
- [2] J.Magueijo, A. Albrecht, D. Coulson, and P. Ferreira, astro-ph/9511042, submitted to *Phy.Rev.Lett.*
- [3] M. White, D. Scott and J. Silk, *Annu. Rev. Atron. Astrophys.* **32** 319-370 (1994).
- [4] L.Knox, *Phys.Rev.* **D52** 4307 (1995).
- [5] G. Jungman, M. Kamionkowski, A. Kosowsky and D. Spergel, astro-ph/9507080, to be published in *Phy.Rev.Lett.* (1996);
- [6] M.Hobson and J.Magueijo, Observability of secondary Doppler peaks by cosmic microwave background experiments with small fields, in preparation.
- [7] M. Tegmark, A Method for extracting maximum resolution power spectra from microwave sky maps, MPI-PhT/94-90,astro-ph/94120640.
- [8] M. Hobson et al, 1995, to be published in *MNRAS*.
- [9] J.Bond and G.Efstathiou, *MNRAS* **226** 655 (1987).
- [10] J.Peebles, *Ap.J.* **185** 413 (1973).
- [11] K.M.Gorski, *Ap.J.* **430** L85 (1994).
- [12] J.Magueijo, *Phys.Rev. D* **52** 4361 (1995).
- [13] D.Scott, M.Srednicki, and M.White, *Ap.J.* **421** L-5 (1994).
- [14] Thompson A. R., Moran J. M., Swenson G. W., 1986, *Interferometry and Synthesis in Radio Astronomy*. Wiley, New York.
- [15] E.Keto, The shapes of cross-correlator interferometers, Lawrence Livermore Nat. Lab. Preprint.

- [16] We have used COBE's $Q = 20\mu K$, and $T = 2.726K$.
- [17] M.Tegmark and G.Efstathiou, An Optimal Method for Subtracting Foregrounds from Multi-Frequency CMB Sky Maps, astro-ph/9507009.
- [18] A.Albrecht and B.Wandelt, in preparation.